Published in final edited form as:
Free Radic Biol Med. 2014 June ; 71: 208–220. doi:10.1016/j.freeradbiomed.2014.03.018.

Mitochondrial Aldehyde Dehydrogenase (ALDH2) Accentuates Aging-Induced Cardiac Remodeling and Contractile Dysfunction: Role of AMPK, Sirt1 and Mitochondrial Function

Yingmei Zhang[1,4,*], **Shou-Ling Mi**[2,3,*], **Nan Hu**[1], **Thomas A. Doser**[1], **Aijun Sun**[2,3], **Junbo Ge**[2,3], and **Jun Ren**[1,2]

[1]Center for Cardiovascular Research and Alternative Medicine, University of Wyoming College of Health Sciences, Laramie, WY 82071 USA

[2]Shanghai Institute of Cardiovascular Diseases, Zhongshan Hospital, Fudan University, Shanghai 200032, P.R. China

[3]Institutes of Biomedical Sciences, Fudan University, Shanghai 200032, P.R. China

[4]Department of Cardiology, Xijing Hospital, Fourth Military Medical University, Xi'an, China 710032

Abstract

Cardiac aging is associated with compromised myocardial function and morphology although the underlying mechanism remains elusive. ALDH2, an essential mitochondrial enzyme governing cardiac function, displays polymorphism in human. This study was designed to examine the role of ALDH2 in aging-induced myocardial anomalies. Myocardial mechanical and intracellular Ca^{2+} properties were examined in young (4–5 mo) and old (26–28 mo) wild-type (WT) and ALDH2 transgenic mice. Cardiac histology, mitochondrial integrity, O_2^- generation, apoptosis and signaling cascades including AMPK activation and Sirt1 level were evaluated. Myocardial function and intracellular Ca^{2+} handling were compromised with advanced aging, the effects were accentuated by ALDH2. H&E and Masson trichrome staining revealed cardiac hypertrophy and interstitial fibrosis associated with greater left ventricular mass and wall thickness in aged mice. ALDH2 accentuated aging-induced cardiac hypertrophy but not fibrosis. Aging promoted O_2^- release, apoptosis and mitochondrial injury (mitochondrial membrane potential, levels of UCP2 and PGC-1α), the effects were also exacerbated by ALDH2. Aging dampened AMPK phosphorylation and Sirt1, the effects of which were exaggerated by ALDH2. Treatment of the ALDH2 activator Alda-1 accentuated aging-induced O_2^- generation and mechanical dysfunction

Correspondence to: Dr. Jun Ren or Dr. Yingmei Zhang, Center for Cardiovascular Research and Alternative Medicine, University of Wyoming College of Health Sciences, Laramie, WY 82071, Tel: (307) 766-6131; Fax: (307) 766-2953; jren@uwyo.edu; zhangym197951@126.com.
*These two authors contributed equally to this work

Competing interests: The authors have declared that no competing interests exist.

in cardiomyocytes, the effects of which were mitigated by co-treatment with activators of AMPK and Sirt1 AICAR, resveratrol and SRT1720. Examination of human longevity revealed a positive correlation between lifespan and ALDH2 gene mutation. Taken together, our data revealed that ALDH2 enzyme may accentuate myocardial remodeling and contractile dysfunction in aging possibly through AMPK/Sirt1-mediated mitochondrial injury.

Keywords

ALDH2; aging; cardiac geometry; contractile function; AMPK; Sirt1

INTRODUCTION

Aging is an irreversible biological process characterized by adaptive changes in the heart including increased left ventricular wall thickness and chamber size, change in diastolic filling pattern such as prolonged diastole, cardiac fibrosis and decreased myocardial contractile capacity, which contribute to increased incidence of morbidity and mortality in the elderly [1, 2]. Although a number of theories were postulated for cardiac aging such as short telomere defect, myosin heavy chain isozyme switch, mitochondrial damage, oxidative stress, impaired intracellular Ca^{2+} handling and excitation-contraction coupling [3–6], the precise mechanism behind cardiac aging remains elusive. Furthermore, aging-related alterations in cardiac geometry and function may be heavily influenced by gender, race and ethnicity [7]. Genetic factors are believed to contribute to an estimated 18% of heart failure incidence [8]. Gene and ethnicity may account for unfavorable changes in high density lipoprotein cholesterol and cardiovascular morbidity in human [9].

The mitochondrial isoform of aldehyde dehydrogenase (ALDH2) is a human gene found on chromosome 12. All Caucasians are homozygous for ALDH2 while nearly 50% of Asians are heterozygous and possess one normal copy of the ALDH2 gene and one mutant copy encoding an inactive mitochondrial isozyme [10]. The ALDH2 inactivating mutation (termed ALDH2*2) is the most common single point mutation in humans with proven epidemiological evidence suggesting a correlation between this inactivating mutation and increased propensity for common human pathologies such as Fanconi anemia, pain, osteoporosis and aging process [11]. For example, epidemiological data revealed a reduced risk of alcoholism in Asians compared with Caucasians, possibly due to alcohol intolerance [10, 12]. A recent meta-analysis of genome-wide association studies has identified a tight association between the ALDH2 mutation and elevated blood pressure in Asian decedents [13]. Furthermore, ample clinical and experimental evidence has depicted a pivotal role of ALDH2 in cardiac homeostasis under both physiological and pathological conditions [11, 14–19]. Findings from our laboratory and others favor a unique role of ALDH2 in the regulation of cardiac homeostasis in diabetes mellitus, alcoholism, endoplasmic reticulum stress, arrhythmias and ischemia-reperfusion injury [14, 15, 20–24]. However, the role of ALDH2 or ALDH2 gene polymorphism in cardiac aging process has not been elucidated. To this end, this study was designed to examine the impact of ALDH2 on cardiac aging and the underlying mechanism(s) involved with a focus on mitochondrial integrity and oxidative stress. To better elucidate the role of mitochondrial integrity, oxidative stress and associated

cell signaling cascades in cardiac aging and/or ALDH2-induced responses, AMPK and the longevity regulator Sirt1 were examined in wild-type (WT) FVB and ALDH2 transgenic mice at young and old age. Furthermore, effect of pharmacological activation of ALDH2, AMPK and Sirt1 was evaluated in young and aged WT mice. Finally, the association between longevity and ALDH2 gene polymorphism was examined in human subjects.

METHODS AND MATERIALS

ALDH2 mice and in vivo drug treatment

The animal experimental procedures described here were approved by our Institutional Animal Care and Use Committee at the University of Wyoming (Laramie, WY, USA). Production of ALDH2 overexpression transgenic mice using the chicken β-actin promoter was described [21]. Four to five month-old (young) and 26–28 month-old (old) male ALDH2 mice and wild-type (WT) littermates were maintained with a 12/12-light/dark cycle with free access to tap water. At the time of sacrifice, blood glucose levels were measured using a glucose meter. To evaluate the effect of activation of ALDH2, AMPK and Sirt1 on cardiac aging, a cohort of young (4–5 month-old) and old WT (or ALDH2 transgenic) mice (26–28 month-old) were treated with the ALDH2 activator Alda-1 (20 mg/kg, i.p., twice per week) [25] in the presence or absence of the AMPK activator 5-aminoimidazole-4-carboxamide-1-β-D-ribofuranoside (AICAR, 0.5 mg/g, i.p. twice per week) [26], the mixed AMPK/Sirt1 activator resveratrol (5 mg/kg, i.p., twice per week) [27] or the small molecule Sirt1 activator SRT1720 (100 mg/kg, gavage, twice per week) [28, 29] for 4 weeks prior to assessment of cardiomyocyte O_2^- production and contractile function.

Human ALDH2 polymorphism

Three hundred and ninety-seven microbian aged between 90 and 107 with an average age of 92.61 ± 2.49 years were enrolled. Three hundred and forty-four healthy individuals from the same region without family history of longevity (> 90 years) were recruited as controls. All subjects were from Zhangqiu, Shandong, China with a nomadic way of life. The experimental protocol was approved by the Fudan University Ethics Committee. All subjects were given informed consent to participate in the study. Individuals with secondary hypertension, diabetes mellitus, or severe liver, and kidney dysfunction were excluded. Three milliliters peripheral venous blood was drawn into sodium citrate solution, and genomic DNA was extracted by a Genomic DNA Purification kit. A 25-μl reaction mixture including 5 μl DNA, 12.5 μl TaqMan PCR master mix, 1.25 μl primers and probes, 6.25 μl deionized water was placed in a real-time PCR instrument (Applied Biosystems, Foster City, CA, USA). The reaction conditions were as the following: initial denaturation at 95°C for 10 min, followed by 40 cycles of denaturation at 92°C for 15 sec and annealing and extension at 60°C for 90 sec [30].

Echocardiographic assessment

Cardiac geometry and function were evaluated in anesthetized (ketamine 80 mg/kg and xylazine 12 mg/kg, i.p.) mice using the 2-D guided M-mode echocardiography (Phillips Sonos 5500) equipped with a 15-6 MHz linear transducer. Left ventricular (LV) anterior and posterior wall dimensions during diastole and systole were recorded from three consecutive

cycles in M-mode using method adopted by the American Society of Echocardiography. Fractional shortening was calculated from LV end-diastolic (ESD) and end-systolic (ESD) diameters using the equation (EDD-ESD)/EDD. Heart rates were averaged over 10 cycles [21].

Isolation of mouse cardiomyocytes

Hearts were mounted onto a temperature-controlled (37°C) Langendorff system. After perfusion with a modified Tyrode's solution, the heart was digested with a Ca^{2+}-free KHB buffer containing liberase blendzyme 4 (Hoffmann-La Roche Inc., Indianapolis, IN) for 20 min. The modified Tyrode solution (pH 7.4) contained the following (in mM): NaCl 135, KCl 4.0, $MgCl_2$ 1.0, HEPES 10, NaH_2PO4 0.33, glucose 10, butanedione monoxime 10, and the solution was gassed with 5% CO_2–95% O_2. The digested heart was then removed from the cannula and left ventricle was cut into small pieces in the modified Tyrode's solution. Tissue pieces were gently agitated and pellet of cells was resuspended. A yield of 60–70% viable rod-shaped cardiomyocytes with clear sacromere striations was achieved. Only rod-shaped myocytes with clear edges were selected for contractile and intracellular Ca^{2+} studies [21].

Cell shortening/relengthening

Mechanical properties of cardiomyocytes were assessed using a SoftEdge MyoCam® system (IonOptix Corporation, Milton, MA, USA) [21]. Cells were placed in a Warner chamber mounted on the stage of an inverted microscope (Olympus, IX-70) and superfused (~1 ml/min at 25 °C) with a buffer containing (in mM): 131 NaCl, 4 KCl, 1 $CaCl_2$, 1 $MgCl_2$, 10 glucose, 10 HEPES, at pH 7.4. The cells were field stimulated with supra-threshold voltage at a frequency of 0.5 Hz (unless otherwise stated), 3 msec duration. The myocyte being studied was displayed on the computer monitor using an IonOptix MyoCam camera. An IonOptix SoftEdge software was used to capture changes in cell length during shortening and relengthening. Cell shortening and relengthening were assessed using the following indices: peak shortening (PS), time-to-PS (TPS), time-to-90% relengthening (TR_{90}), maximal velocities of shortening (+ dL/dt) and relengthening (− dL/dt). In the case of altering stimulus frequency from 0.1 to 5.0 Hz, the steady state contraction of myocyte was achieved (usually after the first 5–6 beats) before PS was recorded.

Intracellular Ca^{2+} transient

Myocytes were loaded with fura-2/AM (0.5 μM) for 10 min and fluorescence measurements were recorded with a dual-excitation fluorescence photomultiplier system (IonOptix). Cardiomyocytes were placed on an Olympus IX-70 inverted microscope and imaged through a Fluor × 40 oil objective. Cells were exposed to light emitted by a 75W lamp and passed through either a 360 or a 380 nm filter, while being stimulated to contract at 0.5 Hz. Fluorescence emissions were detected between 480 and 520 nm after first illuminating the cells at 360 nm for 0.5 sec then at 380 nm for the duration of the recording protocol (333 Hz sampling rate). The 360 nm excitation scan was repeated at the end of the protocol and qualitative changes in intracellular Ca^{2+} concentration were inferred from the ratio of fura-2 fluorescence intensity (FFI) at two wavelengths (360/380). Fluorescence decay time was

measured as an indication of the intracellular Ca^{2+} clearing rate. Both single and bi-exponential curve fits were applied to calculate the intracellular Ca^{2+} decay constant [21].

Intracellular fluorescence measurement of O_2^-

Intracellular O_2^- was measured by changes in fluorescence intensity resulting from intracellular probe oxidation. In brief, cardiomyocytes were loaded with dihydroethidium (DHE, 5 μM) (Molecular Probes, Eugene, OR) for 30 min at 37°C for detection of O_2^-. Cells were sampled randomly using an Olympus BX-51 microscope equipped with Olympus MagnaFire™ SP digital camera and ImagePro image analysis software (Media Cybernetics, Silver Spring, MD, USA). Fluorescence was calibrated with InSpeck microspheres (Molecular Probes). An average of 100 cells was evaluated using the grid crossing method in 15 visual fields per isolation [31].

Histological examination

Following anesthesia, hearts were excised and immediately placed in 10% neutral-buffered formalin at room temperature for 24 hrs after a brief rinse with PBS. The specimen were embedded in paraffin, cut in 5 μm sections and stained with hematoxylin and eosin (H&E). Cardiomyocyte cross-sectional areas were calculated on a digital microscope (×400) using the Image J (version1.34S) software. The Masson's trichrome staining was used to detect fibrosis in heart sections. The percentage of fibrosis was calculated using the histogram function of the photoshop software. Briefly, random fields from each section were assessed for fibrosis. The fraction of light blue stained area normalized to the total area was used as an indicator of myocardial fibrosis [21].

TUNEL assay

TUNEL staining of myonuclei positive for DNA strand breaks were determined using a fluorescence detection kit (Roche, Indianapolis, IN, USA) and fluorescence microscopy. Paraffin-embedded sections (5 μm) were incubated with Proteinase K solution for 30 min. TUNEL reaction mixture containing terminal deoxynucleotidyl transferase (TdT) and fluorescein-dUTP was added to the sections in 50-μl drops and incubated for 60 min at 37°C in a humidified chamber in the dark. The sections were rinsed three times in PBS for 5 min each. Following embedding, sections were visualized with an Olympus BX-51 microscope equipped with an Olympus MaguaFire SP digital camera. DNase I and label solution were used as positive and negative controls. To determine the percentage of apoptotic cells, micrographs of TUNEL-positive and DAPI-stained nuclei were captured using an Olympus fluorescence microscope and counted using the ImageJ software (ImageJ version 1.43r; NIH) from 10 random fields at 400× magnification At least 100 cells were counted in each field [31].

Caspase-3 assay

Tissue homogenates were centrifuged (10,000 *g* at 4°C, 10 min) and pellets were lysed in an ice-cold cell lysis buffer. The assay was carried out in a 96-well plate with each well containing 30 μl cell lysate, 70 μl of assay buffer (50 mM HEPES, 0.1% CHAPS, 100 mM NaCl, 10 mM DTT and 1 mM EDTA) and 20 μl of caspase-3 colorimetric substrate Ac-

DEVD-pNA. The 96-well plate was incubated at 37°C for 1 hr, during which time the caspase in the sample was allowed to cleave the chromophore p-NA from the substrate molecule. Caspase-3 activity was expressed as picomoles of pNA released per μg of protein per min [21].

Mitochondrial membrane potential

Cardiomyocytes were suspended in HEPES-saline buffer and mitochondrial membrane potential ($\Delta\Psi_m$) was detected as described [31]. Briefly, after incubation with JC-1 (5 μM) for 10 min at 37°C, cells were rinsed twice by sedimentation using the HEPES saline buffer free of JC-1 before being examined under a confocal laser scanning microscope (Leica TCS SP2) at excitation wavelength of 490 nm. The emission of fluorescence was recorded at 530 nm (monomer form of JC-1, green) and at 590 nm (aggregate form of JC-1, red). Results in fluorescence intensity were expressed as 590-to-530-nm emission ratio. The mitochondrial uncoupler carbonyl cyanide m-chlorophenylhydrazone (CCCP, 10 μM) was used as a positive control for mitochondrial membrane potential measurement.

Western blot analysis

Murine heart tissues were homogenized and sonicated in a lysis buffer containing 20 mM Tris (pH 7.4), 150 mM NaCl, 1 mM EDTA, 1 mM EGTA, 1% Triton, 0.1% sodium dodecyl sulfate (SDS), and a protease inhibitor cocktail. Samples were incubated with anti-AMPK, anti-phosphorylated AMPK (pAMPK, Thr^{172}), anti-Sit1, anti-UCP-2, anti-peroxisome proliferator-activated receptor coactivator-1α (PGC-1α) and anti-GAPDH (loading control) antibodies. The membranes were incubated with horseradish peroxidase (HRP)-coupled secondary antibodies. After immunoblotting, the film was scanned and detected with a Bio-Rad Calibrated Densitometer and the intensity of immunoblot bands was normalized to that of GAPDH [21].

Data analysis

Data were Mean ± SEM. Statistical significance ($p < 0.05$) was estimated by one-way analysis of variation (ANOVA) followed by a Tukey's test for *post hoc* analysis.

RESULTS

General biometric and echocardiographic characteristics in mice

Biometric data of young or old WT and ALDH2 mice are shown in Table 1. ALDH2 overexpression failed to elicit notable effect on body and organ (heart, liver and kidney) weights compared with the age-matched WT mice. Aged WT and ALDH2 mice displayed heavier body and organ weights (although not organ size) compared with their young counterparts. Neither aging nor ALDH2 or both altered fasting blood glucose levels. Assessment of echocardiographic properties revealed that aging but not ALDH2 increased ventricular wall thickness, the effect of which was more pronounced in aged ALDH2 mice. Neither aging nor ALDH2 transgene affected ESD, EDD and fractional shortening although the aged ALDH2 mice displayed overtly increased ESD (but not EDD) diameter along with lower fractional shortening. Heart rate and cardiac output were not significantly affected by either aging or ALDH2 overexpression.

Cardiomyocyte intracellular Ca^{2+} transient properties

To explore the possible mechanism of action behind the interplay between cardiac aging and ALDH2, intracellular Ca^{2+} handling was evaluated using Fura-2 fluorescence. Our data depicted that neither aging nor ALDH2 significantly affected resting intracellular Ca^{2+} levels. Aging but not ALDH2 significantly decreased electrically-stimulated rise in intracellular Ca^{2+} (ΔFFI) and intracellular Ca^{2+} clearance (single or bi-exponential) with a more pronounced response in ALDH2 overexpression mice (Fig. 1A–D).

Effect of increasing stimulation frequency on cardiomyocyte shortening amplitude

Rodent hearts normally contract at very high frequencies (> 300), whereas our recording was performed at 0.5 Hz. To evaluate the impact of aging and/or ALDH2 overexpression on cardiac contractile function under higher frequencies, we increased the stimulus frequency up to 5.0 Hz (300 beats/min) and recorded steady-state PS amplitude. Cardiomyocytes were initially stimulated at 0.5 Hz to ensure a steady-state before commencing the frequency response. Fig. 1E displays a negative staircase of PS with increasing stimulus frequency in all mice with a steeper decline in aged mice. Although ALDH2 itself failed to elicit any obvious effect on the pattern of frequency-shortening response, it exacerbated aging-induced decline in PS amplitude. These data favor a possible role of compromised intracellular Ca^{2+} cycling and stress tolerance in ALDH2-exacerbated mechanical anomalies in aging.

Effect of ALDH2 overexpression and aging on myocardial histology

To assess the impact of ALDH2 on aging-induced myocardial histological changes, cardiomyocyte cross-sectional area and interstitial fibrosis were examined. H&E and Masson Trichrome staining analyses revealed overtly increased cardiomyocyte transverse cross-sectional area and interstitial fibrosis in aged mouse hearts. While ALDH2 failed to affect cardiomyocyte cross-sectional area and interstitial fibrosis early on, it significantly accentuated aging-induced increase in cardiomyocyte size without affecting aging-associated interstitial fibrosis (Fig. 2).

Effects of ALDH2 on aging-induced O_2^- production, apoptosis and mitochondrial damage

To examine the mechanism(s) behind ALDH2-elicited responses in cardiac anomalies in aging, O_2^- production, apoptosis and mitochondrial integrity were examined in myocardium or cardiomyocytes from young or old WT and ALDH2 mice using TUNEL staining, caspase-3 assay and JC-1 fluorescence microscopy, respectively. Results shown in Fig. 3 depict significantly elevated O_2^- production and TUNEL apoptosis in aged WT mice, with a more pronounced response in aged ALDH2 mice. This is supported by caspase-3 assay. ALDH2 transgene itself did not affect myocardial O_2^- production and apoptosis. Our fluorescence data revealed loss of mitochondrial membrane potential in cardiomyocytes from aged WT mice, the effect of which was accentuated by ALDH2 with little effect by itself. These findings indicate a corroborative role of O_2^- production, apoptosis and mitochondrial function in ALDH2-induced exacerbation of cardiac mechanical and intracellular Ca^{2+} responses in aging.

Effect of aging and ALDH2 transgene on AMPK activation, Sirt1 and mitochondrial proteins

To elucidate possible mechanisms of action behind aging and/or ALDH2-induced cardiac derangements, levels of AMPK, the longevity regulator Sirt1 and mitochondrial proteins (UCP-2 and PGC-1α) were examined. Aging significantly suppressed AMPK phosphorylation, as well as downregulated levels of Sirt1, UCP-2 and PGC-1α, with a more pronounced response in the aged ALDH2 mouse hearts. ALDH2 transgene itself failed to alter the levels of AMPK, pAMPK, Sirt1, UCP-2 and PGC-1α. Neither aging nor ALDH2 significantly affected total protein levels of AMPK (Fig. 4).

Effects of the ALDH2 activator Alda-1, the AMPK activator AICAR, the AMPK/Sirt1 activator resveratrol and the Sirt1 activator SRT1720 on cardiomyocyte dysfunction in aging

To better elucidate a cause-effect relationship among AMPK, Sirt1 and ALDH2 in aging-induced cardiac dysfunction, a cohort of young (4–5 month-old) and old WT mice (26–28 month-old) were treated with the ALDH2 activator Alda-1 (20 mg/kg, i.p., twice per week) [25] in the presence or absence of the AMPK activator AICAR (0.5 mg/g, i.p. twice per week) [26], the mixed AMPK/Sirt1 activator resveratrol (5 mg/kg, i.p., twice per week) [27] or the small molecule Sirt1 activator SRT1720 (100 mg/kg, gavage, twice per week) [28, 29] for 4 weeks prior to assessment of cardiomyocyte O_2^- production and contractile function. Our data shown in Fig. 5 revealed that Alda-1 treatment exacerbated aging-induced cardiomyocyte O_2^- production and mechanical dysfunction without eliciting any notable effect in cardiomyocytes from young mice. Interestingly, the Alda-1-induced unfavorable effects in cardiomyocyte O_2^- production and contractile function were overtly alleviated or obliterated by AICAR, resveratrol and SRT1720. In addition, these pharmacological activators rescued against aging-induced cardiac stress and mechanical anomalies without eliciting any notable effects in young mice (data not shown). These data favor a permissive role for AMPK and Sirt1 in ALDH2 activation-accentuated cardiomyocyte stress and mechanical dysfunction in aging.

Effect of the AMPK/Sirt1 activator resveratrol on ALDH2-induced cardiomyocyte contractile responses in aging

To further ascertain the role of AMPK-Sirt1 signaling cascade in ALDH2-accentuated cardiac aging anomalies, a cohort of young (4–5 month-old) and old (26–28 month-old) WT and ALDH2 transgenic mice were treated with the mixed AMPK/Sirt1 activator resveratrol (5 mg/kg, i.p., twice per week) [27] for 4 weeks prior to assessment of cardiomyocyte contractile function. Our data shown in Fig. 6 revealed that ALDH2 transgene overexpression exacerbated aging-induced cardiomyocyte mechanical defect without eliciting any notable effect in cardiomyocytes from young mice, the effect of which was obliterated by resveratrol (in both aged groups). Resveratrol treatment did not elicit any notable effects in young mice (data not shown). These data favor an essential role for the AMPK-Sirt1 signaling cascade in ALDH2-accentuated cardiomyocyte mechanical dysfunction in aging.

ALDH2 Lys504Glu genetic polymorphism and longevity in human

Given that 50% of Asian decedents carry mutant alleles of ALDH2 [*ALDH2*2/1* (G/A) and *ALDH2*2/2* (A/A)] resulted from a single point mutation of the active *ALDH2*1* (G/G) gene [10, 32, 33], genetic polymorphism was evaluated in populations with a family history of longevity. The frequencies of G/G, G/A, and A/A genotypes were 77.6%, 20.9% and 1.5%, respectively, in control group. Interestingly, the frequencies of G/G, G/A, and A/A genotypes were 65.7%, 32.8%, and 1.5%, respectively, in microbian group, depicting a higher frequency of mutant ALDH2 allele in the microbian group. Further analysis revealed that the glutamate genotype frequency was much lower whereas that of lysine genotype was higher in microbian group compared with the controls (Table 2).

DISCUSSION

The salient findings of our study revealed that ALDH2 significantly accentuated aging-induced cardiac hypertrophy, contractile dysfunction, intracellular Ca^{2+} mishandling, oxidative stress and mitochondrial injury. Our data further revealed that AMPK/Sirt1 activation (AICAR, resveratrol and SRT1720) protects against Alda-1-induced cardiomyocyte contractile dysfunction and O_2^- accumulation with aging. This is also supported by the beneficial effect of resveratrol against ALDH2 transgene-accentuated cardiac aging. These findings suggest a permissive role for the AMPK-Sirt1 signaling cascade in ALDH2-accenuated cardiac aging. Data from human study indicated a positive correlation between ALDH2 mutant allele and longevity. These results have collectively prompted for a possible role of ALDH2 and mitochondrial integrity in the regulation of myocardial morphology and function in aging and more importantly, the therapeutic potential for ALDH2 enzyme and mitochondria as targets in the management against cardiac aging.

Unfavorable changes in myocardial morphology and function are common in aged hearts characterized by cardiac hypertrophy, intracellular Ca^{2+} mishandling, compromised contractility and prolonged diastolic duration [4, 5, 34]. Compromised myocardial function and geometry has been demonstrated in senescence, leading to alterations in diastolic filling and ventricular pump capacity [3, 5]. Nonetheless, ejection fraction, the essential measure of left ventricular systolic performance, is preserved during aging, possibly as a result of enlarged end diastolic volume [3, 5]. This is in line with the unchanged fractional shortening capacity from our echocardiographic measurement in aged WT hearts. However, this compensatory machinery was disappeared in aged ALDH2 mice, somewhat consistent with the less favorable effect of ALDH2 gene in human longevity as shown in our study. Our findings also revealed increased ventricular wall thickness with aging but not ALDH2 early on in life. Interestingly, such aging-induced cardiac remodeling was exaggerated by ALDH2 (as well as unmasked enlargement in ESD). This observation, in conjunction with the more prominent changes in heart mass, heart size, cardiomyocyte cross-sectional area and left ventricular fractional shortening in aged ALDH2 mice, favors a prominent unfavorable role of ALDH2 in aging hearts as opposed to younger age. ESD, which is preserved in the face of both aging and ALDH2 overexpression, is significantly enhanced with the concurrent aging and ALDH2 overexpression, leading to reduced fractional shortening in aged ALDH2

transgenic mice. The calculated echocardiographic cardiac output remains unchanged in response to aging and ALDH2 transgenic expression. Although a precise explanation cannot be offered for such inconsistent findings between fractional shortening and cardiac output, potential compensatory hemodynamic factors may be involved to preserve cardiac output in the face of aging and ALDH2 overexpression. Cardiac hypertrophy and interstitial fibrosis are common manifestations of aging heart and may lead to heart failure [35]. Our data revealed that aged ALDH2 hearts possess greater heart mass, heart size and cardiomyocyte size (although with similar interstitial fibrosis) compared with WT littermates. Although ALDH2 transgene itself did not alter cardiac geometry and function early on, it accentuated advanced aging-elicited echocardiographic and cardiomyocyte mechanical dysfunction. It is noteworthy that ALDH2 accentuated myocardial O_2^- production in the absence of interstitial fibrosis in aging. The disparate finding between O_2^- production and interstitial fibrosis in aged ALDH2 hearts may be related to possible contributions of other free radicals to interstitial fibrosis and the existence of a potential "ceiling response of O_2^-" for myocardial fibrosis.

In our hands, aged murine cardiomyocytes displayed unchanged resting intracellular Ca^{2+} levels, decreased intracellular Ca^{2+} release in response to electrical stimulus and compromised intracellular Ca^{2+} clearance, in line with our previous reports [4, 36, 37]. Although ALDH2 transgene did not affect intracellular Ca^{2+} homeostasis in young mice, it unveiled a dampened release of intracellular Ca^{2+} and decrease in intracellular Ca^{2+} clearance with aging. These findings depict that ALDH2 overexpression with time is capable of disrupting intracellular Ca^{2+} handling. Existence of aging-associated intracellular Ca^{2+} mishandling is further supported by the reduced stress tolerance shown as the steeper negative staircase in frequency response. It was perceived that dampened SERCA2a expression and/or enhanced phospholamban levels may account for, at least in part, intracellular Ca^{2+} mishandling, prolonged intracellular Ca^{2+} clearance and cardiac relaxation in senescent hearts [38] although further investigation is warranted. The fact that ALDH2 failed to affect myocardial contractile and intracellular Ca^{2+} properties in young hearts indicates that overexpression of this enzyme early on in life is not innately harmful to cardiac function.

Several mechanisms may be proposed for ALDH2-elicited exaggeration of aging-induced cardiac mechanical and intracellular Ca^{2+} anomalies. First, our data revealed that ALDH2 augmented aging-induced oxidative stress (O_2^- production) and apoptosis. This is accompanied by dephosphorylation of AMPK and loss of Sirt1. A possible role of AMPK and Sirt1 in ALDH2- and aging-induced cardiac responses was substantiated by the findings that AICAR, resveratrol or SRT1720 effectively negated Alda-1 accentuated cardiomyocyte contractile dysfunction and stress in aging. This is further supported by the beneficial effect of resveratrol against ALDH2-accentuated cardiomyocyte aging. These data favor the notion that ALDH2, with time, promotes oxidative stress and triggers cardiac geometric and functional anomalies during aging. Suppression of AMPK phosphorylation has been reported in aging [39]. Reduction in AMPK phosphorylation in aging with a more pronounced effect in ALDH2 mice as seen in our study should provide a possible explanation for downregulation of Sirt1. This is supported by the ability of resveratrol and SRT1720 to reverse aging-induced (ALDH2 or Alda-1-exacerbated) cardiomyocyte

dysfunction. Sirt1 is a conserved nicotinamide adenine dinucleotide (NAD^+)-dependent protein deacetylase to participate in energy metabolism via deacetylation of its target proteins, including mitochondrial proteins PGC1α and UCP-2 [40]. AMPK, on the other hand, enhances Sirt1 activity through increasing cellular NAD^+ levels, resulting in deacetylation and modulation of the activity of downstream targets of Sirt1 including PGC1α [41]. Our data revealed favorable responses from the mixed AMPK/Sirt1 activator resveratrol and the synthetic Sirt1 activator SRT1720 in ALDH2 or Alda-1-induced cardiac aging responses, supporting a key role of the AMPK/Sirt1 signaling cascade in ALDH2-accenuated cardiac aging. Resveratrol and other Sirt1 activating compounds have shown some promising effects in a number of age-related diseases including cancer, type 1 and type 2 diabetes, inflammation, cardiovascular disease, stroke, hepatic steatosis [42]. Although the precise nature of Sirt1 in ALDH2-regulated cardiac aging process is beyond the scope of our current study, its possible role in the regulation of telomere length should not be underestimated. Moreover, ALDH2 is an enzyme using NAD^+ as a cofactor. This creates a natural "competition for NAD^+" between ALDH2 and the longevity regulator Sirt1, a NAD^+-dependent deacetylases. In consequence, metabolic/energy homeostatic processes relying on NAD^+ availability such as aging may be affected in a negative way by ALDH2 although further scrutiny is warranted with regards to the role of NAD^+ in ALDH2-accenuated cardiac aging process. Last but not the least, the lack of change in blood glucose in aged groups suggest little role of glucose metabolism in ALDH2-accentuated cardiac anomalies.

In summary, our finding suggests that ALDH2 enzyme is capable of accentuating cardiac remodeling and contractile function in the elderly. Our data favor the notion that changes in the AMPK-Sirt1 signaling cascade in aging seems to be responsible for ALDH2-accentuated loss of mitochondrial integrity and apoptosis in aging, indicating the therapeutic potential of ALDH2 and mitochondria as targets in the management of aging-associated cardiac anomalies. ALDH2 polymorphism has been considered an essential risk factor for cardiovascular diseases such as hypertension [13]. Paradoxically, the G/G (Glu/Glu) wild genotype of ALDH2 is also suggested to be an independent risk factor for hypertension [43]. In our hands, ALDH2 mutant alleles are found to be positively correlated with longevity. Although our study sheds some light on the role of AMPK activation and Sirt1 in the regulation of ALDH2- and aging-induced cardiac geometric, functional and intracellular Ca^{2+} changes, the pathogenesis of cardiac dysfunction under aging especially in association with mitochondrial integrity deserves further investigation.

Acknowledgments

This work was supported in part by NIH P20 RR016474, GM103432 and the Natural Science Foundation of China 81200102.

REFERENCES

1. Dutta D, Calvani R, Bernabei R, Leeuwenburgh C, Marzetti E. Contribution of impaired mitochondrial autophagy to cardiac aging: mechanisms and therapeutic opportunities. Circ Res. 2012; 110:1125–1138. [PubMed: 22499902]

2. Strait JB, Lakatta EG. Aging-associated cardiovascular changes and their relationship to heart failure. Heart Fail Clin. 2012; 8:143–164. [PubMed: 22108734]

3. Lakatta EG. Cardiovascular aging research: the next horizons. J Am Geriatr Soc. 1999; 47:613–625. [PubMed: 10323658]

4. Yang X, Doser TA, Fang CX, Nunn JM, Janardhanan R, Zhu M, Sreejayan N, Quinn MT, Ren J. Metallothionein prolongs survival and antagonizes senescence-associated cardiomyocyte diastolic dysfunction: role of oxidative stress. FASEB J. 2006; 20:1024–1026. [PubMed: 16585059]

5. Yang X, Sreejayan N, Ren J. Views from within and beyond: narratives of cardiac contractile dysfunction under senescence. Endocrine. 2005; 26:127–137. [PubMed: 15888924]

6. Armanios M, Blackburn EH. The telomere syndromes. Nature reviews. Genetics. 2012; 13:693–704.

7. Smith NL, Felix JF, Morrison AC, Demissie S, Glazer NL, Loehr LR, Cupples LA, Dehghan A, Lumley T, Rosamond WD, Lieb W, Rivadeneira F, Bis JC, Folsom AR, Benjamin E, Aulchenko YS, Haritunians T, Couper D, Murabito J, Wang YA, Stricker BH, Gottdiener JS, Chang PP, Wang TJ, Rice KM, Hofman A, Heckbert SR, Fox ER, O'Donnell CJ, Uitterlinden AG, Rotter JI, Willerson JT, Levy D, van Duijn CM, Psaty BM, Witteman JC, Boerwinkle E, Vasan RS. Association of genome-wide variation with the risk of incident heart failure in adults of European and African ancestry: a prospective meta-analysis from the cohorts for heart and aging research in genomic epidemiology (CHARGE) consortium. Circ Cardiovasc Genet. 2010; 3:256–266. [PubMed: 20445134]

8. Lee DS, Pencina MJ, Benjamin EJ, Wang TJ, Levy D, O'Donnell CJ, Nam BH, Larson MG, D'Agostino RB, Vasan RS. Association of parental heart failure with risk of heart failure in offspring. N Engl J Med. 2006; 355:138–147. [PubMed: 16837677]

9. Rhoades DA, Welty TK, Wang W, Yeh F, Devereux RB, Fabsitz RR, Lee ET, Howard BV. Aging and the prevalence of cardiovascular disease risk factors in older American Indians: the Strong Heart Study. J Am Geriatr Soc. 2007; 55:87–94. [PubMed: 17233690]

10. Peng GS, Yin SJ. Effect of the allelic variants of aldehyde dehydrogenase ALDH2*2 and alcohol dehydrogenase ADH1B*2 on blood acetaldehyde concentrations. Hum Genomics. 2009; 3:121–127. [PubMed: 19164089]

11. Chen CH, Ferreira JC, Gross ER, Mochly-Rosen D. Targeting aldehyde dehydrogenase 2: new therapeutic opportunities. Physiological reviews. 2014; 94:1–34. [PubMed: 24382882]

12. Zhang Y, Ren J. ALDH2 in alcoholic heart diseases: molecular mechanism and clinical implications. Pharmacol Ther. 2011; 132:86–95. [PubMed: 21664374]

13. Kato N, Takeuchi F, Tabara Y, Kelly TN, Go MJ, Sim X, Tay WT, Chen CH, Zhang Y, Yamamoto K, Katsuya T, Yokota M, Kim YJ, Ong RT, Nabika T, Gu D, Chang LC, Kokubo Y, Huang W, Ohnaka K, Yamori Y, Nakashima E, Jaquish CE, Lee JY, Seielstad M, Isono M, Hixson JE, Chen YT, Miki T, Zhou X, Sugiyama T, Jeon JP, Liu JJ, Takayanagi R, Kim SS, Aung T, Sung YJ, Zhang X, Wong TY, Han BG, Kobayashi S, Ogihara T, Zhu D, Iwai N, Wu JY, Teo YY, Tai ES, Cho YS, He J. Meta-analysis of genome-wide association studies identifies common variants associated with blood pressure variation in east Asians. Nat Genet. 2011; 43:531–538. [PubMed: 21572416]

14. Chen CH, Sun L, Mochly-Rosen D. Mitochondrial aldehyde dehydrogenase and cardiac diseases. Cardiovascular research. 2010; 88:51–57. [PubMed: 20558439]

15. Budas GR, Disatnik MH, Mochly-Rosen D. Aldehyde dehydrogenase 2 in cardiac protection: a new therapeutic target? Trends Cardiovasc Med. 2009; 19:158–164. [PubMed: 20005475]

16. Zhang H, Gong DX, Zhang YJ, Li SJ, Hu S. Effect of mitochondrial aldehyde dehydrogenase-2 genotype on cardioprotection in patients with congenital heart disease. European heart journal. 2012; 33:1606–1614. [PubMed: 22507973]

17. Fan F, Sun A, Zhao H, Liu X, Zhang W, Jin X, Wang C, Ma X, Shen C, Zou Y, Hu K, Ge J. MicroRNA-34a promotes cardiomyocyte apoptosis post myocardial infarction through down-regulating aldehyde dehydrogenase 2. Current pharmaceutical design. 2013; 19:4865–4873. [PubMed: 23323620]

18. Ferreira JC, Mochly-Rosen D. Nitroglycerin use in myocardial infarction patients. Circulation journal : official journal of the Japanese Circulation Society. 2012; 76:15–21. [PubMed: 22040938]
19. Gu C, Xing Y, Jiang L, Chen M, Xu M, Yin Y, Li C, Yang Z, Yu L, Ma H. Impaired cardiac SIRT1 activity by carbonyl stress contributes to aging-related ischemic intolerance. PLoS One. 2013; 8:e74050. [PubMed: 24040162]
20. Chen CH, Budas GR, Churchill EN, Disatnik MH, Hurley TD, Mochly-Rosen D. Activation of aldehyde dehydrogenase-2 reduces ischemic damage to the heart. Science. 2008; 321:1493–1495. [PubMed: 18787169]
21. Doser TA, Turdi S, Thomas DP, Epstein PN, Li SY, Ren J. Transgenic overexpression of aldehyde dehydrogenase-2 rescues chronic alcohol intake-induced myocardial hypertrophy and contractile dysfunction. Circulation. 2009; 119:1941–1949. [PubMed: 19332462]
22. Ma H, Guo R, Yu L, Zhang Y, Ren J. Aldehyde dehydrogenase 2 (ALDH2) rescues myocardial ischaemia/reperfusion injury: role of autophagy paradox and toxic aldehyde. European heart journal. 2011; 32:1025–1038. [PubMed: 20705694]
23. Zhang B, Zhang Y, La Cour KH, Richmond KL, Wang X, Ren J. Mitochondrial aldehyde dehydrogenase obliterates endoplasmic reticulum stress-induced cardiac contractile dysfunction via correction of autophagy. Biochimica et biophysica acta. 2013
24. Koda K, Salazar-Rodriguez M, Corti F, Chan NY, Estephan R, Silver RB, Mochly-Rosen D, Levi R. Aldehyde dehydrogenase activation prevents reperfusion arrhythmias by inhibiting local renin release from cardiac mast cells. Circulation. 2010; 122:771–781. [PubMed: 20697027]
25. Ding X, Beier JI, Baldauf KJ, Jokinen JD, Zhong H, Arteel GE. Acute ethanol preexposure promotes liver regeneration after partial hepatectomy in mice by activating ALDH2. American journal of physiology. Gastrointestinal and liver physiology. 2013
26. Cieslik KA, Taffet GE, Crawford JR, Trial J, Mejia Osuna P, Entman ML. AICAR-dependent AMPK activation improves scar formation in the aged heart in a murine model of reperfused myocardial infarction. J Mol Cell Cardiol. 2013; 63:26–36. [PubMed: 23871790]
27. Kanamori H, Takemura G, Goto K, Tsujimoto A, Ogino A, Takeyama T, Kawaguchi T, Watanabe T, Morishita K, Kawasaki M, Mikami A, Fujiwara T, Fujiwara H, Seishima M, Minatoguchi S. Resveratrol reverses remodeling in hearts with large, old myocardial infarctions through enhanced autophagy-activating AMP kinase pathway. The American journal of pathology. 2013; 182:701–713. [PubMed: 23274061]
28. Bellet MM, Nakahata Y, Boudjelal M, Watts E, Mossakowska DE, Edwards KA, Cervantes M, Astarita G, Loh C, Ellis JL, Vlasuk GP, Sassone-Corsi P. Pharmacological modulation of circadian rhythms by synthetic activators of the deacetylase SIRT1. Proceedings of the National Academy of Sciences of the United States of America. 2013; 110:3333–3338. [PubMed: 23341587]
29. Fan H, Yang HC, You L, Wang YY, He WJ, Hao CM. The histone deacetylase, SIRT1, contributes to the resistance of young mice to ischemia/reperfusion-induced acute kidney injury. Kidney international. 2013; 83:404–413. [PubMed: 23302720]
30. Hasi T, Hao L, Yang L, Su XL. Acetaldehyde dehydrogenase 2 SNP rs671 and susceptibility to essential hypertension in Mongolians: a case control study. Genet Mol Res. 2011; 10:537–543. [PubMed: 21476199]
31. Zhang Y, Li L, Hua Y, Nunn JM, Dong F, Yanagisawa M, Ren J. Cardiac-specific knockout of ETA receptor mitigates low ambient temperature-induced cardiac hypertrophy and contractile dysfunction. J Mol Cell Biol. 2012; 4:97–107. [PubMed: 22442497]
32. Yin SJ, Peng GS. Acetaldehyde, polymorphisms and the cardiovascular system. Novartis Found Symp. 2007; 285:52–63. discusion 63-58, 198-199. [PubMed: 17590986]
33. Nishimura FT, Fukunaga T, Kajiura H, Umeno K, Takakura H, Ono T, Nishijo H. Effects of aldehyde dehydrogenase-2 genotype on cardiovascular and endocrine responses to alcohol in young Japanese subjects. Auton Neurosci. 2002; 102:60–70. [PubMed: 12492137]
34. Kudo N, Barr AJ, Barr RL, Desai S, Lopaschuk GD. High rates of fatty acid oxidation during reperfusion of ischemic hearts are associated with a decrease in malonyl-CoA levels due to an increase in 5'-AMP-activated protein kinase inhibition of acetyl-CoA carboxylase. J Biol Chem. 1995; 270:17513–17520. [PubMed: 7615556]

35. Wei JY. Age and the cardiovascular system. N Engl J Med. 1992; 327:1735–1739. [PubMed: 1304738]

36. Li Q, Ren J. Influence of cardiac-specific overexpression of insulin-like growth factor 1 on lifespan and aging-associated changes in cardiac intracellular Ca2+ homeostasis, protein damage and apoptotic protein expression. Aging cell. 2007; 6:799–806. [PubMed: 17973971]

37. Li Q, Wu S, Li SY, Lopez FL, Du M, Kajstura J, Anversa P, Ren J. Cardiac-specific overexpression of insulin-like growth factor 1 attenuates aging-associated cardiac diastolic contractile dysfunction and protein damage. Am J Physiol Heart Circ Physiol. 2007; 292:H1398–H1403. [PubMed: 17085535]

38. Ceylan-Isik AF, Dong M, Zhang Y, Dong F, Turdi S, Nair S, Yanagisawa M, Ren J. Cardiomyocyte-specific deletion of endothelin receptor A rescues aging-associated cardiac hypertrophy and contractile dysfunction: role of autophagy. Basic research in cardiology. 2013; 108:335. [PubMed: 23381122]

39. Li Q, Ceylan-Isik AF, Li J, Ren J. Deficiency of insulin-like growth factor 1 reduces sensitivity to aging-associated cardiomyocyte dysfunction. Rejuvenation Res. 2008; 11:725–733. [PubMed: 18729805]

40. Sauve AA, Wolberger C, Schramm VL, Boeke JD. The biochemistry of sirtuins. Annual review of biochemistry. 2006; 75:435–465.

41. Canto C, Gerhart-Hines Z, Feige JN, Lagouge M, Noriega L, Milne JC, Elliott PJ, Puigserver P, Auwerx J. AMPK regulates energy expenditure by modulating NAD+ metabolism and SIRT1 activity. Nature. 2009; 458:1056–1060. [PubMed: 19262508]

42. Hubbard BP, Sinclair DA. Small molecule SIRT1 activators for the treatment of aging and age-related diseases. Trends in pharmacological sciences. 2014

43. Hui P, Nakayama T, Morita A, Sato N, Hishiki M, Saito K, Yoshikawa Y, Tamura M, Sato I, Takahashi T, Soma M, Izumi Y, Ozawa Y, Cheng Z. Common single nucleotide polymorphisms in Japanese patients with essential hypertension: aldehyde dehydrogenase 2 gene as a risk factor independent of alcohol consumption. Hypertens Res. 2007; 30:585–592. [PubMed: 17785925]

Research highlights

- We examined the effect of ALDH2 in cardiac aging;
- ALDH2 accentuates aging-induced cardiac remodeling and dysfunction;
- The unfavorable effect of ALDH2 was related to dampened AMPK-Sirt1 signaling;

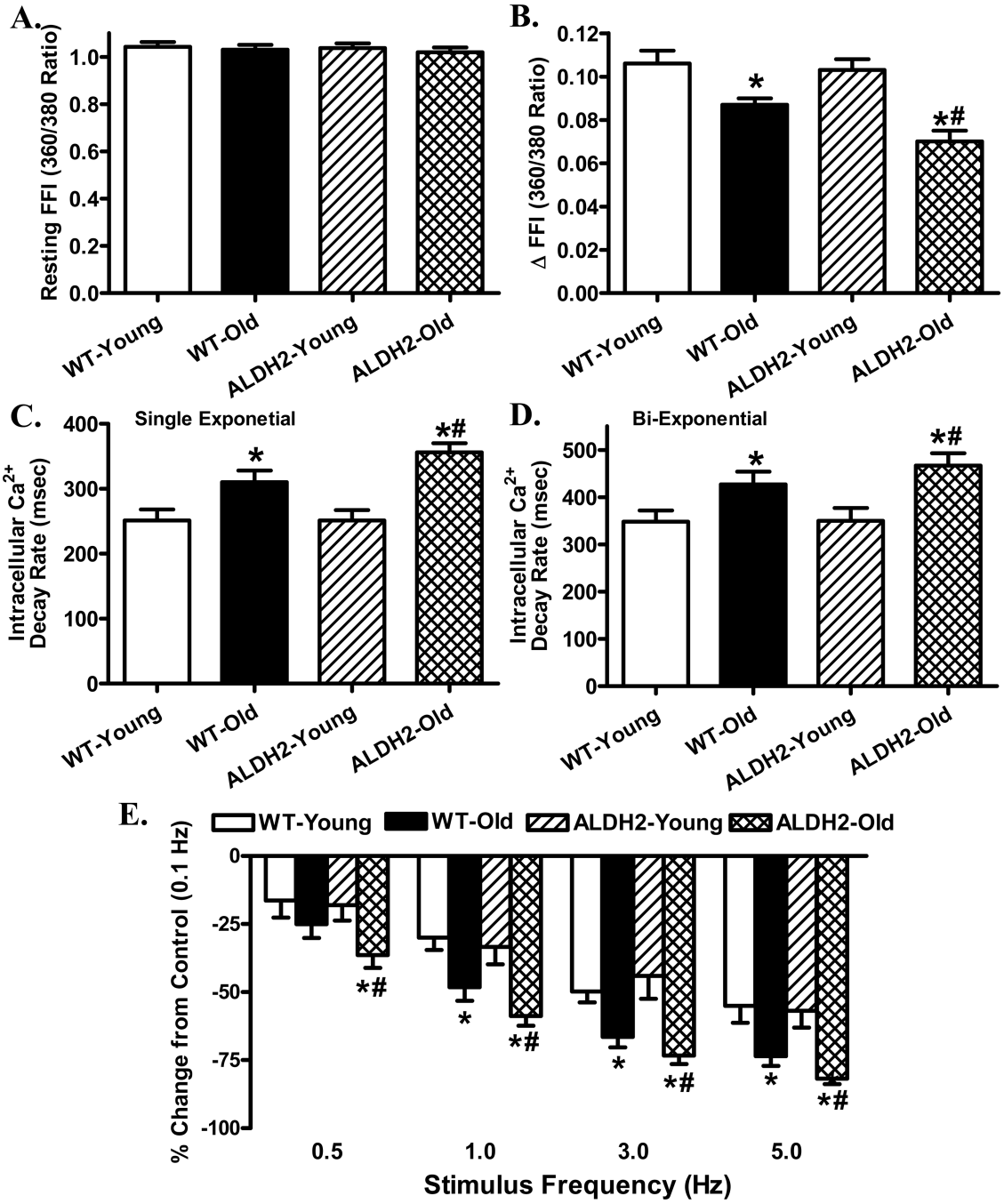

Fig. 1.

Intracellular Ca^{2+} and frequency response in cardiomyocytes from young or old WT and ALDH2 transgenic mice. A: Resting fura-2 fluorescence intensity (FFI); B: Electrically-stimulated rise in FFI (ΔFFI); C: Single exponential intracellular Ca^{2+} decay; D: Bi-exponential intracellular Ca^{2+} decay; and E: Changes in peak shortening of cardiomyocytes (normalized to that obtained at 0.1 Hz from the same cell) at various stimulus frequencies (0.1 – 5.0 Hz). Mean ± SEM, n = 65 cells (panels A–D) and 22 – 28 cells (panel E) from 5 mice per group, * $p < 0.05$ *vs.* WT-young group, # $p < 0.05$ *vs.* WT-old group.

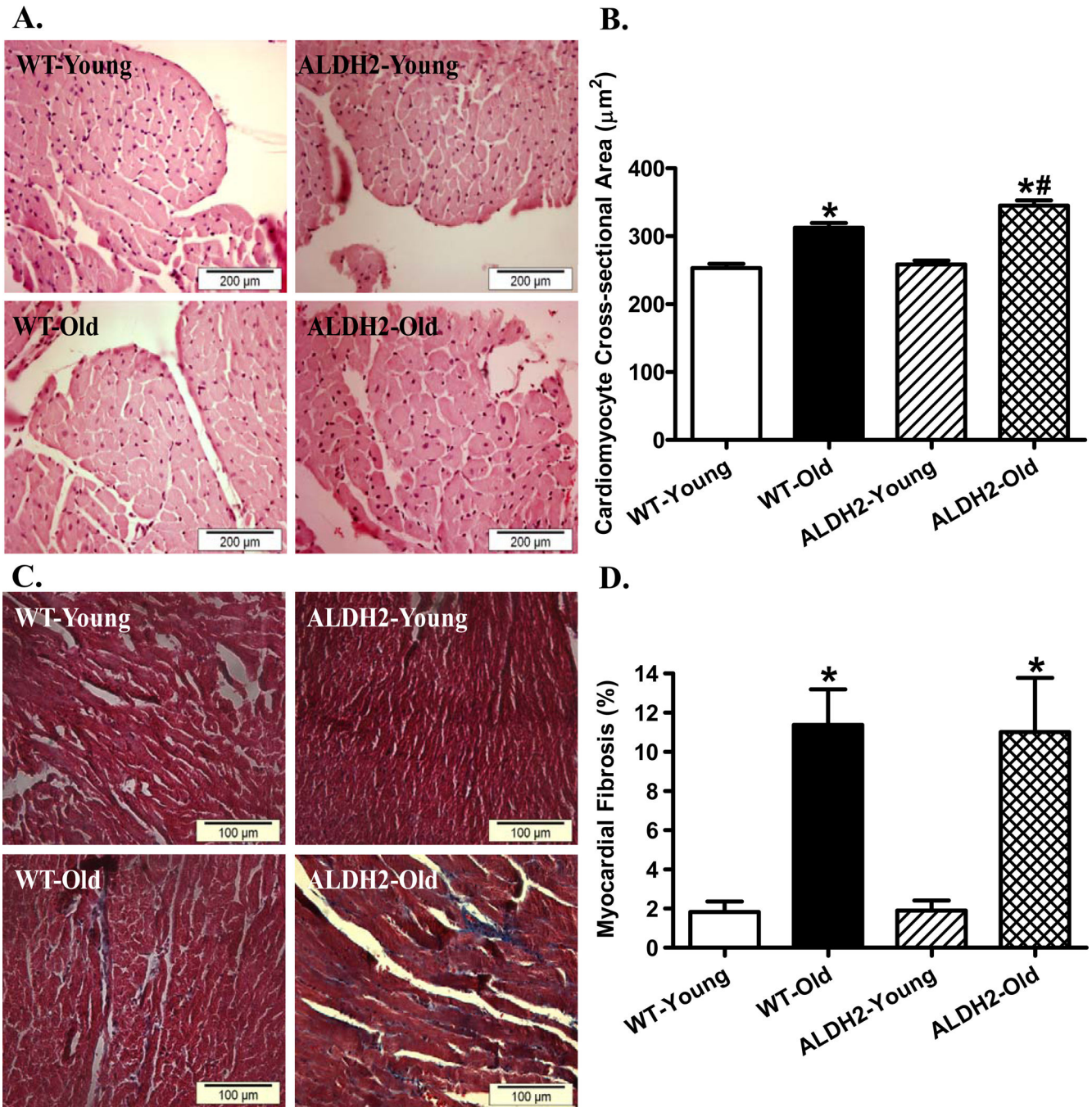

Fig. 2.

Histological analysis in hearts from young or old WT and ALDH2 transgenic mice. A: Representative H&E staining micrographs displaying transverse myocardial section (× 400); B: Quantitative analysis of cardiomyocyte cross-sectional (transverse) area; C: Masson trichrome staining micrographs displaying interstitial fibrosis (× 400); and D: Quantitative analysis of interstitial fibrosis (shown as percent fibrotic area); Mean ± SEM, n = 188 – 217 cells (pane A) and 16–19 fields (panel C) from 4 mice per group * $p < 0.05$ *vs.* WT-young group, # $p < 0.05$ *vs.* WT-old group.

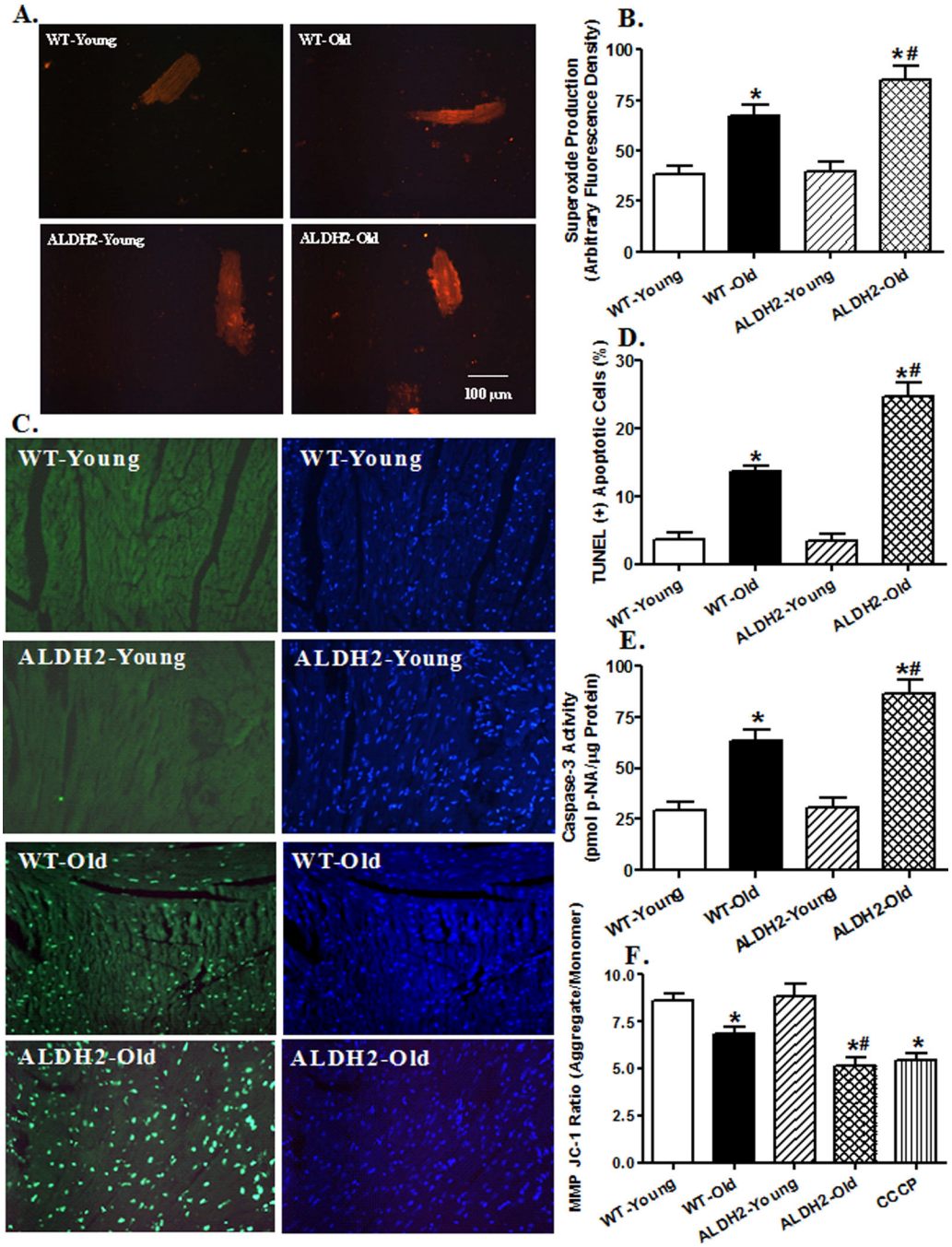

Fig. 3.

Effect of aging and ALDH2 on myocardial O_2^- production, apoptosis and mitochondrial membrane potential (MMP). A: Representative DHE images (400×) showing O_2^- production in cardiomyocytes from young or old WT and ALDH2 mice; B: Pooled data of O_2^- production from 14–15 fields (4 mice/group); C: Representative TUNEL staining depicting myocardial apoptosis. All nuclei were stained with DAPI (blue) while TUNEL-positive nuclei were visualized with fluorescence (green). Original magnification = 400 ×; D: Quantified TUNEL apoptosis shown as % TUNEL positive cells from 12 fields per

group; E: Myocardial apoptosis measured using Caspase-3 activity from 5–6 mice/group; and F: Quantitative analysis of cardiomyocyte MMP using JC-1 fluorescence from 7 fields (3 mice per group, 10 μM CCCP was used as positive control); Mean ± SEM, *$p < 0.05$ *vs.* WT-young group; # $p < 0.05$ *vs.* WT-old group.

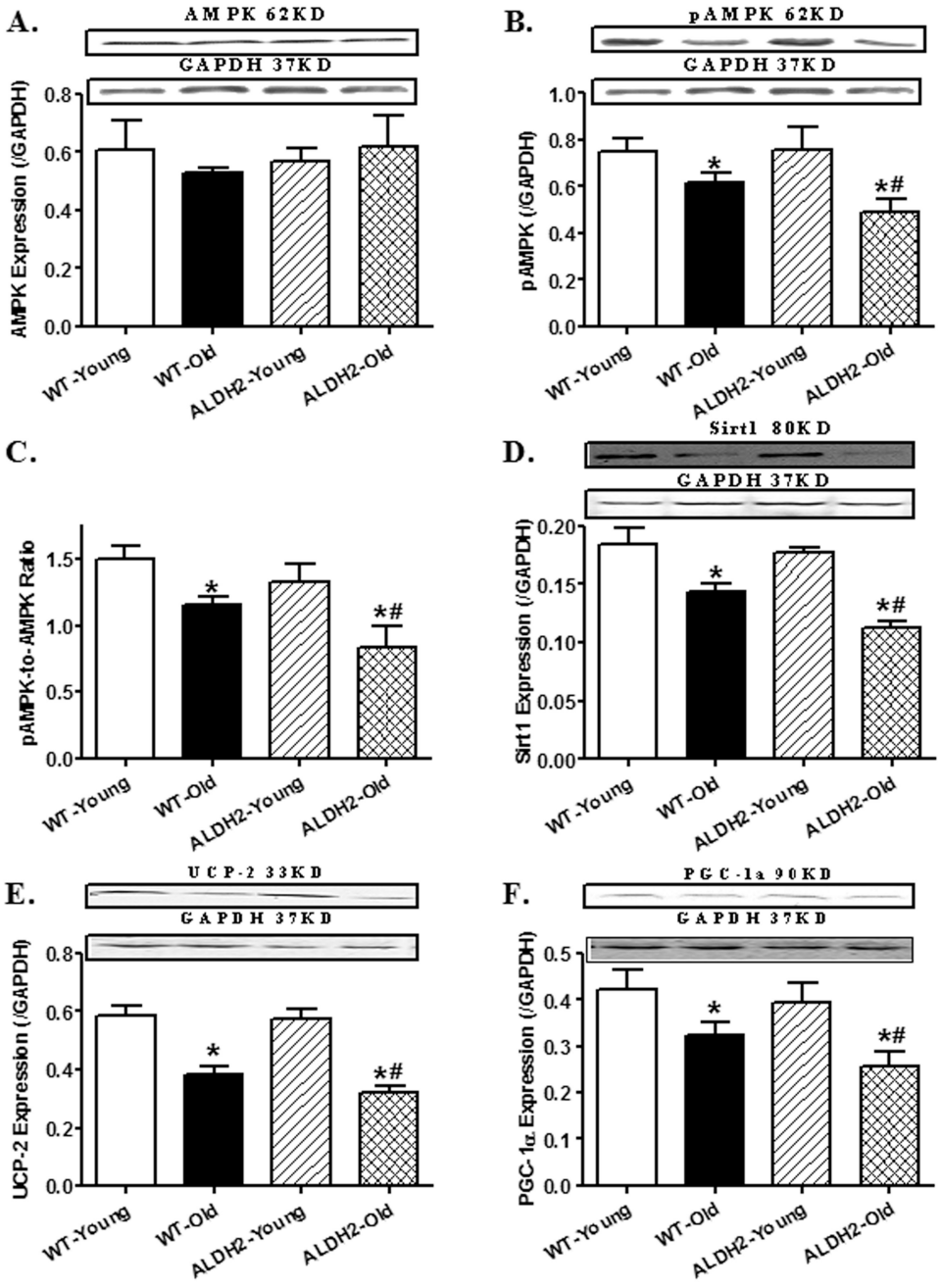

Fig. 4.

Effect of aging and ALDH2 on levels of AMPK, Sirt1 and mitochondrial proteins (UCP-2 and PGC-1α). A: AMPK; B: phosphorylated AMPK (pAMPK, Thr^{172}); C: pAMPK-to-AMPK ratio; D: Sirt1; E: UCP-2; and F: PGC-1α. Insets: Representative gel blots for levels of AMPK, phosphorylated AMPK, Sirt1, UCP-2, PGC-1α and GAPDH (loading control) using specific antibodies; Mean ± SEM, n = 6 – 7 mice per group, * $p < 0.05$ *vs.* WT-young group, # $p < 0.05$ *vs.* WT-old group.

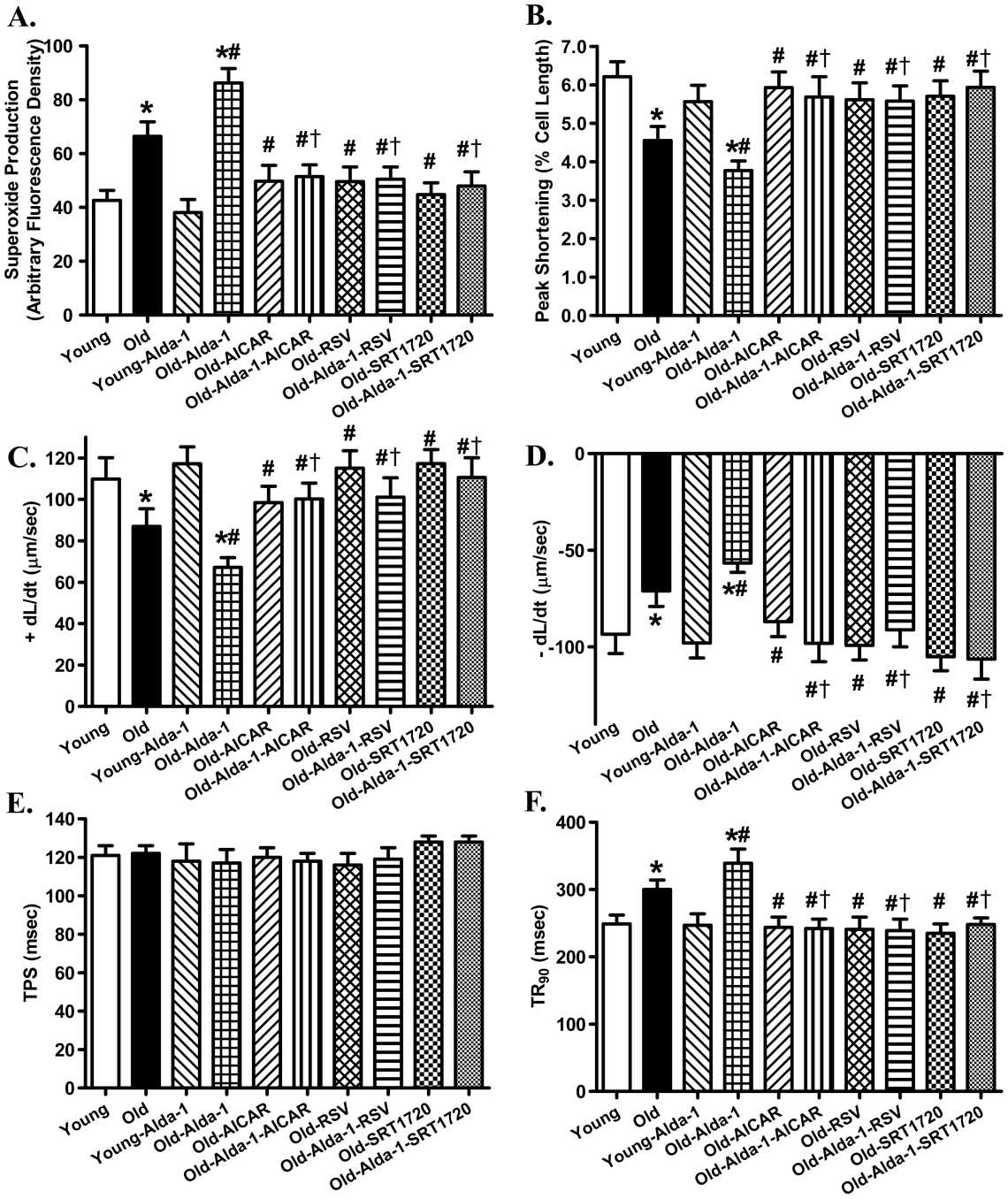

Fig. 5.

Effect of the Alda-1 activator Alda-1 on cardiomyocyte O_2^- production and mechanical properties in young (4–5 month-old) or old (26–28 month-old) mice in the absence or presence of activators of AMPK and Sirt1 (AICAR, resveratrol and SRT1720). Mice were treated with Alda-1 (20 mg/kg, i.p., twice per week) in the presence or absence of the AMPK activator AICAR (0.5 mg/g, i.p. twice per week), the mixed AMPK/Sirt1 activator resveratrol (5 mg/kg, i.p., twice per week) or the Sirt1 activator SRT1720 (100 mg/kg, gavage, twice per week) for 4 weeks prior to assessment of cardiac O_2^- production and

mechanical function. A: O_2^- production; B: Peak shortening (normalized to cell length); C: Maximal velocity of shortening (+ dL/dt); D: Maximal velocity of relengthening (− dL/dt); E: Time-to-PS (TPS); and F: Time-to-90% relengthening (TR_{90}). Mean ± SEM, n = 8 independent isolations (panel A) or 72 cells (panels B–F) per group, *$p < 0.05$ *vs.* Young group, # $p < 0.05$ *vs.* Old group. † $p < 0.05$ *vs.* Old-Alda-1 group.

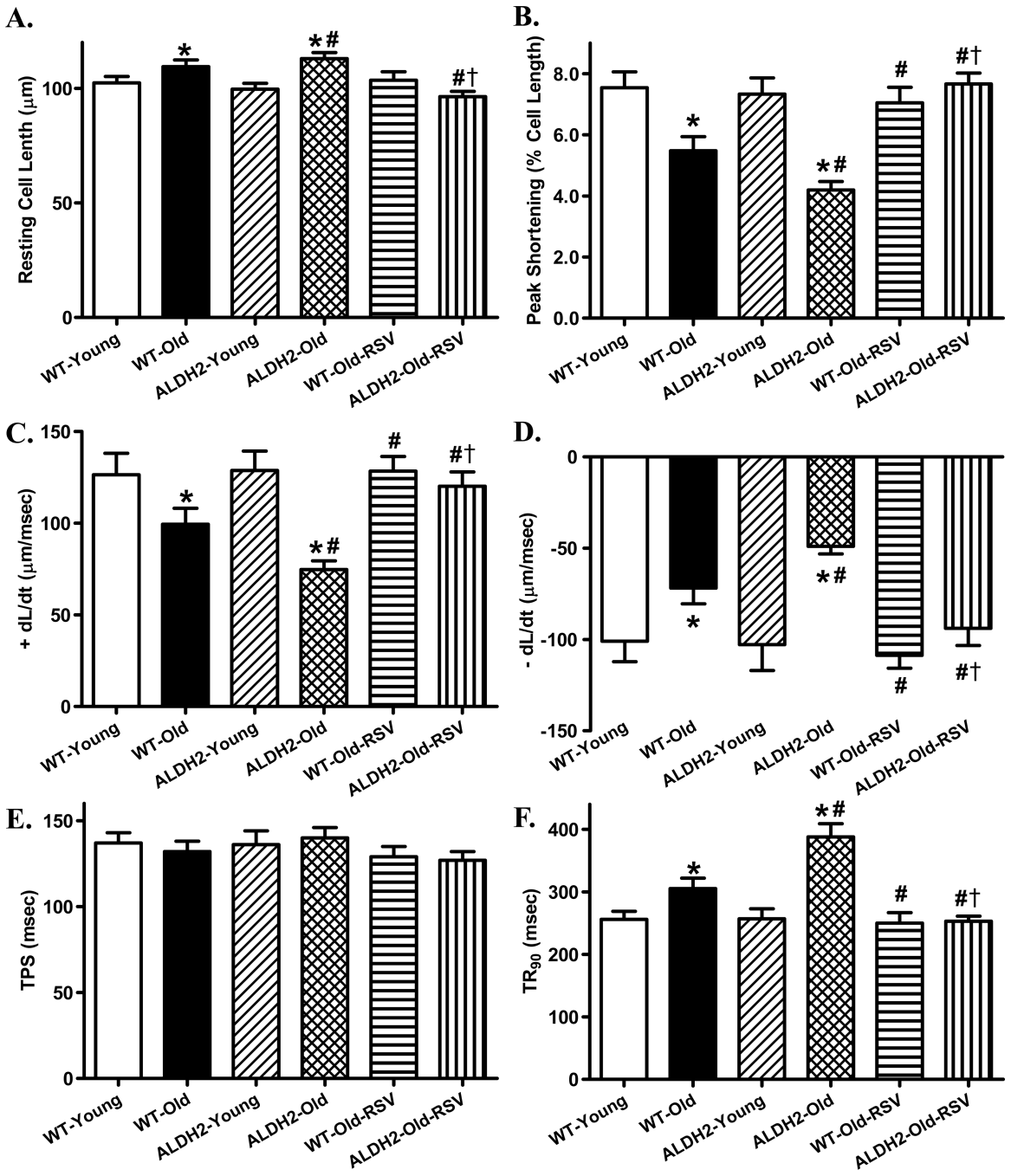

Fig. 6.

Effect of the AMPK/Sirt1 activator resveratrol on cardiomyocyte mechanical function in young (4–5 month-old) or old (26–28 month-old) WT and ALDH2 transgenic mice. Mice were treated with resveratrol (RSV, 5 mg/kg, i.p., twice per week) for 4 weeks prior to assessment of cardiac mechanical properties. A: Resting cell length; B: Peak shortening (normalized to cell length); C: Maximal velocity of shortening (+ dL/dt); D: Maximal velocity of relengthening (− dL/dt); E: Time-to-PS (TPS); and F: Time-to-90%

relengthening (TR_{90}). Mean ± SEM, n = 70 cells per group, *p < 0.05 *vs.* WT-Young group, # p < 0.05 *vs.* WT-Old group. † p < 0.05 *vs.* ALDH2-Old group.

Table 1

Biometric and echocardiographic parameters of WT and ALDH2 transgenic mice

Parameter	WT-Young	WT-Old	ALDH2-Young	ALDH2-Old
Body Weight (g)	26.0 ± 0.8	33.9 ± 2.8*	24.1 ± 0.8	37.1 ± 3.5*
Heart Weight (mg)	139 ± 4	167 ± 12*	134 ± 8	199 ± 13*,#
Heart/Body Weight (mg/g)	5.39 ± 0.21	4.99 ± 0.20	5.54 ± 0.19	5.48 ± 0.20*
Liver Weight (g)	1.36 ± 0.05	1.74 ± 0.13*	1.28 ± 0.08	1.90 ± 0.19*
Liver/Body Weight (mg/g)	52.7 ± 1.9	51.6 ± 1.7	52.6 ± 1.9	51.0 ± 1.0
Kidney Weight (g)	0.33 ± 0.01	0.46 ± 0.05*	0.29 ± 0.02	0.48 ± 0.03*
Kidney/Body Weight (mg/g)	12.6 ± 0.3	13.4 ± 0.6	12.1 ± 0.4	13.2 ± 0.8
Fasting Blood Glucose (mg/dl)	104 ± 5	100 ± 6	98 ± 3	102 ± 5
Heart Rate (bpm)	466 ± 21	463 ± 23	462 ± 25	475 ± 24
Wall Thickness (mm)	0.90 ± 0.06	1.10 ± 0.03*	0.88 ± 0.02	1.22 ± 0.04*,#
EDD (mm)	2.51 ± 0.19	2.54 ± 0.15	2.49 ± 0.16	2.61 ± 0.09
ESD (mm)	1.23 ± 0.13	1.38 ± 0.12	1.25 ± 0.09	1.59 ± 0.07*,#
LV Mass (mg)	69.4 ± 5.7	86.7 ± 7.8*	68.0 ± 5.9	100.9 ± 5.9*,#
Normalized LV Mass (mg/g)	2.43 ± 0.16	2.71 ± 0.22	2.62 ± 0.22	3.05 ± 0.22*
Fractional Shortening (%)	48.4 ± 2.8	46.1 ± 2.3	50.6 ± 1.4	39.6 ± 1.6*,#
Cardiac Output (mm^3/min)	7472 ± 1682	6852 ± 1469	6645 ± 1084	6739 ± 983

HW = heart weight; EDD = end diastolic diameter; ESD = end systolic diameter; LV = left ventricular. Mean ± SEM, n = 10 mice per group,

* $p < 0.05$ *vs.* respective young group,

# $p < 0.05$ *vs.* WT-old group.

Table 2

Association of ALDH2 genetic polymorphisms with longevity in Chinese

ALDH2 (Lys504Glu) Genetic polymorphisms	Control (y < 90)	Macrobian (y ≥ 90)	Odds ratio (95% CI)	P value
Normal Activity G/G)	267/344 (77.6%)	261/397 (65.7%)	1	p < 0.05
Intermediate Activity (G/A)	72/344 (20.9%)	130/397 (32.8%)	0.554 (0.399–0.768)	
Weak Activity (A/A)	5/344 (1.5%)	6/397 (1.5%)		
Phenotypes G	303 88.08%	326 82.12%	1	p < 0.05
A	41 11.92%	71 17.88%	0.621 (0.410–0.941)	